



## THEORETICAL AND PRACTICAL PERSPECTIVES OF DIESEL LOCOMOTIVE WITH DC TRACTION MOTORS WHEEL-SETS' SLIPPING AND SLIDING CONTROL

Lionginas Liudvinavičius<sup>1</sup>, Gintautas Bureika<sup>2</sup>

*Dept of Railway Transport, Vilnius Gediminas Technical University, LT-03224 Vilnius, Lithuania*  
*E-mails: <sup>1</sup>lionginas.liudvinavicius@vgtu.lt; <sup>2</sup>gintautas.bureika@vgtu.lt (corresponding author)*

*Submitted 7 March 2011; accepted 6 September 2011*

**Abstract.** The causes of slipping and sliding of the locomotive's driving wheel-sets are analysed from theoretical and practical perspectives. The main factors influencing wheel-sets' slipping are described, and their correlation is determined. The specific methods of stopping the slipping of the Diesel locomotives and having a conventional electric drive system are described in the paper. The process of wheel-sets' slipping and its control are simulated and shown graphically. Structural diagrams demonstrating the control of the dynamic locomotive wheel-sets' slipping and sliding, based on the evaluation of the influence of the speed-torque characteristics of DC traction motors on these processes, are presented. Major parameters of the DC/DC and AC/DC systems used in the automatic control of the dynamic slipping and sliding of the locomotive's wheel-sets are defined and new methods of controlling the dynamic slipping and sliding are suggested.

**Keywords:** locomotive, traction generator's characteristic, DC traction motor, adhesion coefficient, slip force, slipping and sliding, slip and slide protection system.

### 1. Introduction

The efficiency of transportation by railway largely depends on railway track capacity. A railway operator has to ensure steady and safe traffic, as well as the effective use of the locomotive power. The problems associated with the comfortability of passenger trains were investigated by Inarida *et al.* (2001), while the parameters of electrodynamic braking and power systems of the trains were considered by Liudvinavičius and Lingaitis (2010). To ensure a steady traffic flow of trains (particularly, heavy freight trains), the tractive force of the locomotive should be effectively controlled. It is important to control the locomotive so that its tractive force should be uniformed and its development could not be interrupted because of the driving wheel-sets' sliding. The conditions for the wheel-sets to slide are usually created, when a heavy train starts moving or is moving uphill (Bureika 2008). In this case, the locomotive is moving so that the driving wheels' spin speed sharply increases, while the tractive force of the locomotive decreases fast, causing a sharp slowdown of the straight-line motion of the train, which may even stop between the stations.

When the adhesion coefficient is decreased considerably, the locomotive's tractive force is not sufficient to pull the train. In this case, sand is spread on the rails to

increase the adhesion coefficient. However, the starting time of a locomotive increases due to intense slipping of the wheel-sets, which causes more intense wearing both of the wheel-sets and rails. A number of researchers study the problem of the effective control of the locomotive's tractive force, e.g. Myamlin (2002) and Radojković (1990).

Slipping of the locomotive's wheel-sets depends on the angle of taper of the wheels' rolling surface as well as the slope of the track and the wheel-set position with respect to the longitudinal axis of the rails. When a locomotive is moving in the traction mode, the axle load of the locomotive's powered wheel-sets acting on the rails is redistributed, and this is one of the main causes of slipping and sliding of the wheels.

The effect of the variation of the coefficient of adhesion between the wheels and the rails on the tractive effort characteristic as well as the operation of electric traction motors and the effect of their arrangement in the carriage on the static wheel-to-rail force are also very important. Another relevant problem is the adjustment and control of the parameters of the wheel-sets' slipping and sliding in the case of various types of the locomotive drives, such as DC/DC, AC/DC and the latest type of AC/AC drives. The operation of these drives is de-

scribed in the works of Strekopytov *et al.* (2003), Sen (1996), Liudvinavičius and Lingaitis (2010) and Nayal *et al.* (2006). In order to effectively control slipping and sliding of the DC motor-driven wheel-sets, the mechanical characteristics of motors and the effectiveness of the methods of speed regulation of the rotors of these motors should be determined. The algorithms for automating the control of the electric motors were considered by Yamaguchi (2006).

Assuming that the mechanical characteristics of the DC traction generators may have a certain influence on slipping, the structural control diagrams of the processes of slipping and sliding of the wheels were developed in the course of investigation. Based on the analysis of the main factors contributing to slipping, and, given the parameters of this process, the modelling of wheel-sets' slipping and its control methods was performed.

When the driving wheel-set starts sliding, it makes more revolutions and, theoretically, due to the specific mechanical characteristics of the DC traction generator, the rotor (and the wheel-set) may 'race'. In practice, the process lasts until the mechanical failure of the electrical motor's armature takes place. The more revolutions the wheel makes, the higher is the slipping, while the tractive force of a locomotive drops to zero. The authors investigated the mechanical characteristics of the DC traction in order to find the ways of avoiding the unwanted drop of the tractive force.

## 2. Theoretical Assumptions of the Locomotive Wheel-Sets' Slipping and the Consequences of the Wheel-Sets Sliding on the Track

High adhesion utilisation and sophisticated dynamics design of modern locomotives and traction rolling-stocks demand complex simulations which at the same time take into consideration the mechanical, electro-technical and traction control system field. When the locomotive's tractive force exceeds the adhesion of the wheels to the rails, slipping of the locomotive's wheel-sets may start. In vehicle dynamics, small slip values (microslip) are of the main importance. The correct description of the resulting traction coefficient between wheel and rail is important for investigations related to wear, rolling contact fatigue, traction control or running stability analyses. Furthermore, information about local mechanical and thermal load distributions within the contact zone is desirable. A profound description of the state of the art of dynamical contact problems with friction can be found in (Sextro 2010). Longitudinal and lateral slip as well as spin slip should be taken in account (Polach 2005).

The adhesion coefficient is a variable and it strongly affects traction. The variation of the wheel-to-rail adhesion coefficient  $\Psi$  of the locomotive is given for various seasons in Fig. 1.

To determine the adhesion coefficient of a new locomotive, field tests are carried out in various seasons and in various periods of the day. Several hundred tests should be performed to obtain accurate results. In Fig. 1, it is shown that the adhesion coefficient varies consider-

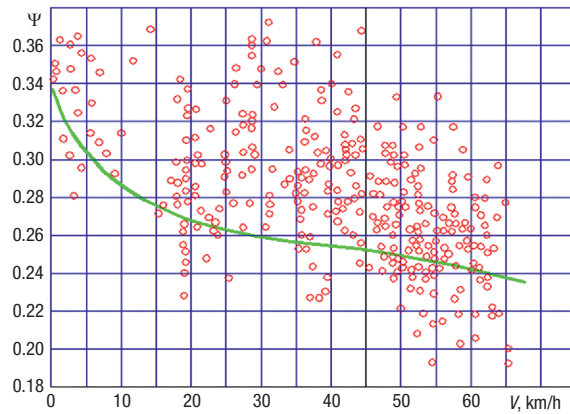


Fig. 1. The variation of the adhesion coefficient  $\Psi$ , depending on the locomotive speed in a particular season

ably, even if the mass of the locomotives is actually the same. It depends on many factors, including rain, snow, the contamination of the rails by the oil products, wearing of the rolling surface of the wheel and the rails, the track profile, etc.

'Conventional' contact models like CONTACT (Kalker 1967), deduced simplifications such as FASTSIM (Kalker 1982) or analytical derivatives of the model (Polach 2005) are able to describe the principal mechanisms linked to the stick and slip zones within the contact rail/wheel and are therefore capable of describing the characteristic correlation between locomotive traction coefficient and slippage. The friction coefficient between wheel and rail has to be provided by the user. This coefficient is highly dependent on parameters such as wheel rolling velocity, normal axle load, microscopic surface roughness of wheel and rail, etc. Moreover, these parameter influences are strongly dependent on the lubrication state of the contact, whether the contact is humid, i.e. boundary lubricated, dry or in mixed lubrication state, where enough fluid is present between wheel and rail to build up a positive fluid pressure regime.

With emphasis on the lubrication only, sophisticated models for elastic-hydrodynamic lubrication (EHL) have been developed and extended to the application to rough surfaces (Patir, Cheng 1978). These researchers introduced flow factors to averaged Reynolds equations for an application to rough surfaces. This method is applicable to the full and mixed lubrication regime, where the fluid fully occupies the area between the two contacting bodies, causing hydrodynamic lift. The method was applied to isothermal rolling contact and the adhesion coefficient was approximated (Chen *et al.* 2005). A tangential contact model was not employed. A method to use this model even under boundary lubrication conditions is proposed in (Hu, Zhu 2000).

The interfacial fluid model is presented by Tomberger *et al.* (2011) and can be used in combined, mixed and boundary lubricated contacts. A new approach is the consideration of the metallic volume occupation by the surface roughness peaks, called asperities. This interfacial fluid model is based on the continuity equation,

a pressure-mass flow relation and an abstraction of the surface geometry.

A possible explanation of the decreasing of slip force-slip function for large longitudinal slip is the decrease of friction coefficient with increasing slip speed due to the increasing temperature in the rail/wheel contact area (Hou, Kalousek 2000; Ertz, Knothe 2002; Ertz, Bucher 2003). With increasing slip, the temperature in the rail/wheel contact area increases and the coefficient of adhesion decreases.

Another explanation is different friction coefficients in the area of adhesion and the area of slip (static kinematic friction coefficient) – does not seem to influence sufficiently the shape of the slip force curve (Ohyama 1989; Nielsen, Theiler 1996).

The method described by Polach (2005) allows simulating slip force according to measurement for various conditions – dry, wet, contaminated, etc. It is based on fast method for calculation of wheel/rail forces developed by Polach and largely tested and used in various three dimensional multi-body simulation tools.

This method developed by Polach for calculation of slip forces in multi-body simulations (Polach 1992, 1999; Kalker 1982) is based on theoretical model for longitudinal and lateral slip assuming a coefficient characterising the rail/wheel contact shear stiffness.

The rail/wheel contact area is assumed elliptically with half-axes  $a$ ,  $b$  and normal stresses  $\sigma$  distribution according to Hertz. The distribution of tangential stress  $\tau$  is shown in Fig. 2.

The maximum value of tangential stress at any random point is:

$$\tau_{max} = \mu \times \sigma, \tag{1}$$

where:  $\mu$  – coefficient of friction.

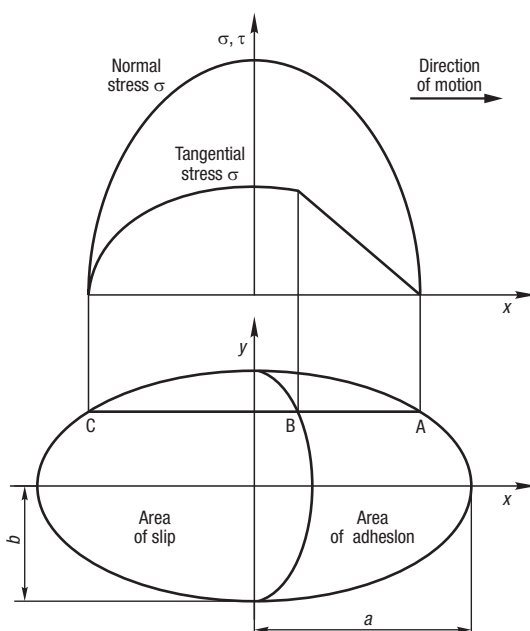


Fig. 2. Distribution of normal and tangential stresses in the rail/wheel contact area in Polach (2005) method

The forces  $F_x, F_y$  in longitudinal and lateral directions are:

$$F_i = F \cdot \frac{s_i}{s}, \quad i = x, y \tag{2}$$

and the adhesion coefficient:

$$f_i = \frac{F_i}{Q}, \quad i = x, y, \tag{3}$$

where:  $F_i$  – total contact force, kN;  $s_i$  – total slip;  $Q$  – wheel load, kN.

A slip force law with a marked adhesion optimum can be modelled using the friction coefficient decreasing with increasing slip (creep) speed between rail and wheel (Zhang *et al.* 2002).

In additional, the reduction of the initial gradient of slip force curve explained by Bucher *et al.* (2002) through the influence of the surface roughness and by Harrison *et al.* (2000) in effect of surface's contamination can be used.

A large longitudinal slip between wheel and rail occurs for the adhesion limit, in particular for the maximum transmissible tractive forces. Using the theory of friction coefficient decreasing with increasing slip by the influence of temperature for the case of wet or polluted contact conditions, the only way to achieve the adhesion optimum at large slip values is a significant reduction of the coefficient of Kalker's linear theory (Polach 2005). With increasing slippage, the temperature in the contact area increases and the coefficient of friction decreases.

Typical values of the reduction factor for real rail/wheel contact conditions as evaluated from measurements are  $0.2 \div 0.5$  for wet rails and  $0.6 \div 0.85$  for dry rails. It should be noted that the only use of decreasing adhesion coefficient does not allow simulating the slip forces between wheel and rail in complex dynamics simulations when transmitting the limiting tractive force under unfavourable adhesion conditions. The modelling proposed by Polach (2005) is of the real slip forces for wet, polluted or dry rail which is based on a combination of dry and wet friction.

Large slip occurs mainly on longitudinal direction because of traction or braking; the maximum lateral slip cannot reach the level of maximum longitudinal slip due to the traction or braking.

The definition of the tangential failure stress  $\tau_m$  is, however, difficult. In addition, to the mechanism of adhesion, plastic asperity deformation, plowing and other dissipative mechanisms, boundary lubrication and influences of solid interfacial layers have an effect on the tangential failure stress of a contact. Furthermore, so-called third bodies, forming a solid interface between the contacting bodies, can alter the friction process (Berthier *et al.* 2004; Niccolini, Berthier 2005).

A run on the unstable (decreasing) section of slip force curve was simulated by Polach (2001). With increasing tractive effort, the wheel-set steering ability decreases. Simultaneously, the first wheel-set of the bogie moves to the inner rail.

Measurements under the water lubricated conditions report a distinct decrease of the maximum traction

coefficient with increasing rolling velocities (Zhang *et al.* 2002; Ohyama, Maruyama 1982; Chen *et al.* 2008). No velocity dependence is reported in paper (Ohyama *et al.* 1989) for a boundary lubricated contact, using paraffinic-oil.

Researchers Mei *et al.* (2009) propose a radically new approach for the detection of wheel slip/slide and re-adhesion control of AC traction motors in railway applications, which provides an important alternative and advantageous technique in traction/braking control systems to maximize the use of adhesion in poor rail/wheel contact conditions. The proposed concept explores the variations in the locomotive wheel-set dynamic properties caused by the condition changes at the wheel–rail contact, detects and controls the slip conditions from the dynamic behaviour of a wheel-set, indirectly. The influence of contact conditions on the relevant modes is assessed, which is essential in the development of a mechatronic solution based on dynamic interactions.

At the current stage of development in models described above (also methods presented in books by Andersson *et al.* 2004; Iwnicki 2006; Wickens 2003) can be widely used for investigations relating to the development of locomotives traction (slip and slide) control strategies and rail/wheel wear or rolling contact materials fatigue.

### 3. The Effect of the Speed–Torque Characteristics of the DC Traction Motor of a Locomotive on Slipping and Sliding of the Wheels

#### 3.1. Speed–Torque Characteristics of the Locomotive’s DC Traction Motor

The main principles of electric motor operation and control are described in the book of Sen (1996). Circuit diagrams (series-wound DC traction motor circuit diagram and separately excited shunt-wound DC traction motor circuit diagram) as well as their *speed–torque characteristics* are presented in Figs 3–5.

The variation of the rotor speed of the series-wound and shunt-wound DC traction motors, depending on the axle load, is shown by the curves depicted in Fig. 5.

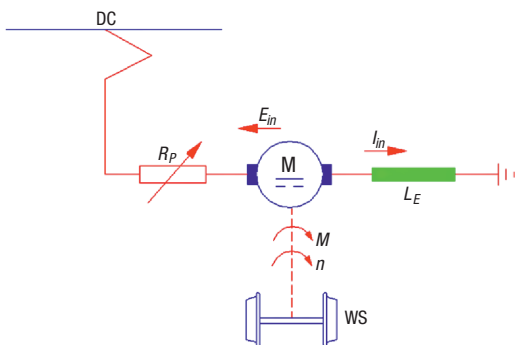


**Fig. 3.** A circuit diagram of a series-wound DC traction motor:  $I_{in}$  is armature current;  $E_{in}$  is armature voltage;  $M$  is the electromagnetic moment in the traction mode;  $n$  is DC motor’s rotor speed;  $L_E$  is an exciting winding; WS denotes wheel-sets;  $R_p$  is the resistor

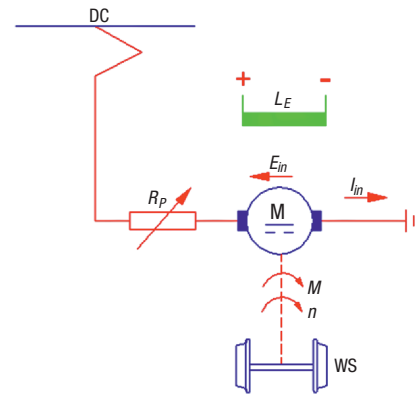


**Fig. 4.** A circuit diagram of a separately excited shunt-wound DC traction motor:  $I_{in}$  is armature current;  $E_{in}$  is armature voltage;  $M$  is the electromagnetic moment in the traction mode;  $n$  is the traction motor’s rotor speed;  $L_E$  is an exciting winding; WS denotes wheel-sets;  $R_p$  is the resistor

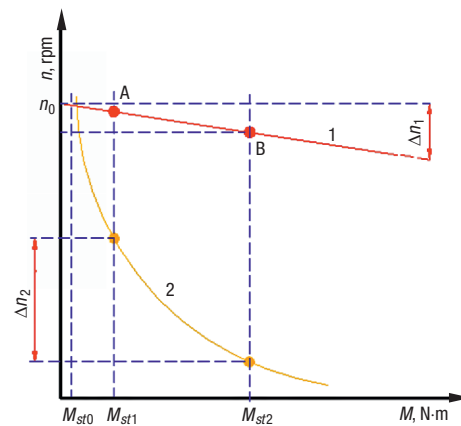


**Fig. 5.** Speed–torque characteristics of the separately excited shunt-wound (1) and series-wound (2) DC traction motors:  $M_{st0}$ ,  $M_{st1}$ ,  $M_{st2}$  denote static load torque of a DC traction motor;  $n_0$  is no-load armature speed of a separately excited shunt-wound DC traction motor

Series-wound DC machines are used as motors and generators. Series-wound traction motors have a very high starting torque. The speed of the DC series-wound motor is strongly dependent on the load. A variation in load causes a variation in current. If the load is increased, the current increases and the speed is reduced. During the start-up and on high load the series-wound traction motor consumes a high current, which produces a powerful torque.

They may never be operated without the load torque because they may ‘race’ on no-load. A series-wound traction motor cannot be operated on no-load under any circumstances because it increases its speed to such a degree that the armature is destroyed, i. e. it ‘races’ on no-load (see Fig. 5).

In a DC series-wound traction motor, operating without the load torque, the rotor speed increases very quickly and the wheel-sets start slipping. The analysis of the speed–torque characteristics of the DC series-wound and separately excited shunt-wound traction

motors at the points A and B allows us to state that the rotor speed of a separately excited shunt-wound traction motor is hardly dependent on the load (speed variation  $\Delta n_1$ ), while speed variation  $\Delta n_2$  of a series-wound DC traction motor is much higher. In addition, as shown in the curve 2 in Fig. 5, a series-wound DC traction motor cannot operate on no-load. Traction motors of the latter type are commonly used in locomotives. When the wheel-to-rail forces are redistributed for the reasons discussed above, the speed of the less heavily loaded wheel increases fast, causing the development of slipping and sliding of the wheel-sets. The locomotives with the DC series-wound traction motors must use anti-slip systems.

### 3.2. Wheel-to-Rail Adhesion of the Locomotives with Separately Excited Shunt-Wound and Series-Wound DC Traction Motors

The authors analyse wheel-to-rail adhesion for the locomotives using separately excited shunt-wound (characteristic 3) and series-wound (characteristic 2) DC traction motors (see Fig. 6). The curve  $F_{ks}$  corresponds to the boundary tractive force characteristic depending on adhesion. At the point A, the boundary tractive force depending on adhesion is found, while the locomotive speed is  $v$ . If the adhesion is weaker, e.g. on the contaminated track section, the tractive force depending on adhesion is decreased by the magnitude  $\Delta F_{ks}$ . Therefore, in this case, the tractive force will be higher than the adhesion force, and the wheel-sets will start slipping and sliding on the track.

When the angle speed of a wheel-set of the locomotive with a separately excited shunt-wound DC traction motor increases, the tractive force of the locomotive sharply decreases, getting equal to the tractive force depending on adhesion at the point B. In this case, the wheel-set's slipping rate  $\Delta v_1$  is low. However, the value of the friction coefficient remains high and, therefore, the wheel-sets, after passing over the reduced adhesion area, will regain the proper adhesion. In a similar case with a series-wound DC traction motor, its tractive force and tractive force depending on adhesion are equal at the point C, where the slipping rate of the wheel-set  $\Delta v_2$  is high, while the friction coefficient is low. In this case, the conditions for regaining the proper adhesion without any external help are much worse. Therefore,

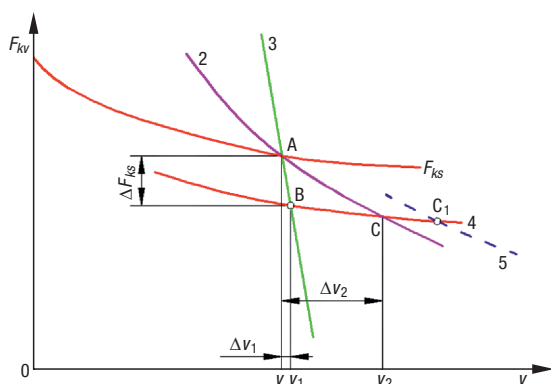


Fig. 6. The effect of speed-torque characteristics on the tractive force of a locomotive depending on adhesion

the spreading of sand in the reduced adhesion area is required for the wheel-sets to regain good adhesion to the rails. The latter is faster regained by the locomotives with separately excited shunt-wound DC tractive motors. Therefore, their average tractive force, depending on adhesion, is higher than that of the series-wound DC traction motors. The locomotives with separately excited shunt-wound DC traction motors have a higher wheel-to-rail adhesion coefficient compared to those having series-wound DC traction motors, whose low adhesion coefficient is compensated for by the use of slipping and skidding protection systems.

## 4. Protecting the Driving Wheel-Sets of a Locomotive from Skidding

### 4.1. A Scheme of the Mechanical Compensating System of Wheel-to-Rail Force Redistribution

In Fig. 7, a scheme of the mechanical compensating system of wheel-to-rail force redistribution for a locomotive operating in the traction mode is given. A system consists of the pneumatic cylinders located perpendicular to the outward wheel-sets of the first and the second bogie. When the locomotive starts moving, the compressed air is supplied to the front cylinders (with respect to the direction of movement), denoted by 1 (Fig. 7), and their shafts squeeze the frames of the bogies. In order to balance the moment  $M_T$ , occurring when the locomotive is moving along the curved track, the first wheel-sets of the respective bogies are pressed. The system is automated, which implies that a special regulator changes the pressure in the system, depending on the tractive force. A pressure regulator is controlled by the pressure relays connected to the network of the traction motors. The higher the current in the network of traction motors and pressure relays, the higher the tractive force of a locomotive and, therefore, the more highly compressed air is supplied to the pneumatic system. Depending on the direction of the locomotive's motion, the valve K1 or K2 is opened. By controlling the position of the valves K1 and K2 and pressure in the cylinders, the forces compensating for the decrease of the axle loads of the bogies are generated. These forces 'press' the bogies to the rails, thereby increasing the adhesion coefficient of the locomotive.

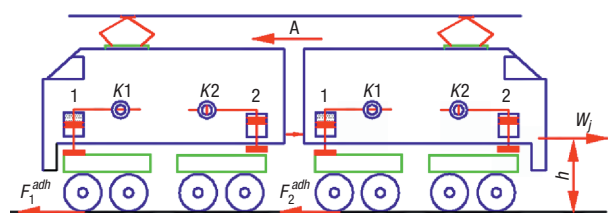


Fig. 7. A scheme of a compensating system of the wheel-to-rail forces' redistribution in a locomotive operating in the traction mode:  $F_1^{adh}$  and  $F_2^{adh}$  are powered wheel tractive efforts;  $W_j$  denotes the resistance tractive effort at the locomotive's automatic coupling;  $h$  is the distance (height) from the rail head to the automatic coupling;  $l$  denotes the hydraulic cylinders; K1, K2 are the valves; A denotes the direction of the locomotive motion

The mechanical system of the wheel-set load compensation is rather complicated. The variation of the axle loads should be controlled by the sensors, while the pressure in particular cylinders should be regulated by the valves. The electric system to protect from slipping and sliding suggested by the authors may supplement the mechanical system of the wheel-set load compensation.

#### 4.2. A Conventional Slip and Slide Protection System for Diesel-Electric (DC/DC) Locomotives

During the slipping and sliding of the powered wheel-sets the adhesion coefficient of the wheel-sets to rails decreases, thereby decreasing the locomotive tractive force. Therefore, the locomotive wheel-sets' adhesion to the rails should be closely watched and adequately controlled to protect them from slipping (Braess, Seiffert 2011).

Usually, the parameters of the locomotive slipping are continually measured and adjusted by specially installed automatic control systems of the electric drives. The main causes of slipping and sliding of the wheel-sets of the locomotives with the DC traction motors connected in series are as follows: redistribution of loads (armature current) due to mismatch of the characteristics of traction motors of the same type and different wheel-to-rail forces in the same locomotive, as well as due to various types of the mechanical characteristic of a traction motor. The mechanical speed-torque characteristic of series-wound DC traction motors used in the DC/DC and AC/DC electric drives is given as the 2nd curve in Fig. 5.

Series-wound DC traction motors described above are widely used in trolley-buses, trams, metro trains, electric trains and locomotives. In practice, the systems of measuring the parameters of wheel slipping or automatic slip and slide protection systems (ACS) are used in the electric drives of the operating traction locomotives.

A conventional circuit diagram of the slip and slide protection system of DC/DC diesel-electric powered locomotive wheel-sets is shown in Fig. 8.

#### 4.3. The Algorithm of Controlling the Locomotive's Wheel-Set Slipping and Sliding

The slipping parameters of each wheel-set may be measured and adjusted by two relays, fixing the slipping process, which is connected between the two armature windings of the traction motor of a bogie. For example,

when the slipping of the first bogie's wheel-sets proceeds, the difference in the potentials at the points of the winding of the relay  $R_{B1}$  can be observed, and the relay works. In this case, the electric circuit is made by the relay's contacts in the lamp indicating slipping or in the bell. A driver is informed about the proceeding slipping by a light or sound signal. Other relay's contacts open the feeding circuit of the contactor  $K$ , thereby interrupting the excitation of the DC traction generator as well as the feeding of the DC traction motors. When the feeding of all traction motors of the operating locomotive is interrupted for a short time, slipping is stopped. The locomotive moving by inertia passes over the section of the greased rails, where the adhesion of the wheel-sets to the rails is particularly weak. If slipping continues, the sand is spread in front of the powered wheel-set wheels to increase the friction. The main disadvantage of the system is that slipping usually does not stop and the driver has to interrupt the traction mode. This causes the development of the horizontal dynamic forces in the train. These dynamic forces may squeeze out some wagons of the train and cause an accident. The authors of the present paper offered to use an automatic drive system of slip and slide protection of the wheel-sets in diesel-electric locomotives (of the DC/DC type). The system's circuit diagram is presented in Fig. 9.

To control automatically the locomotive's slipping, the load characteristic of the traction generator in the dynamic process should be changed. When any of the locomotive wheel-sets starts slipping, the armature current of the traction motors connected in parallel is redistributed, while the voltage at the generator's terminals remains the same (see Fig. 10).

Therefore, the slipping of any wheel-set may be determined by measuring the traction motor's armature current by a current sensor (Program... 2011). A signal for automatic slipping control will be the variation of the traction motor's armature current. The units MCB1 and MCB2 (Fig. 9) measure the armature current of all traction motors by the sensors  $B_1, \dots, B_6$  and determine the maximal current. These signals are compared in the pulse gating unit with the signal obtained by the generator's voltage sensor. The load characteristic of the traction generator changed by the maximal current signal is shown with its dynamic component being formed by a green-coloured curve (Fig. 10).

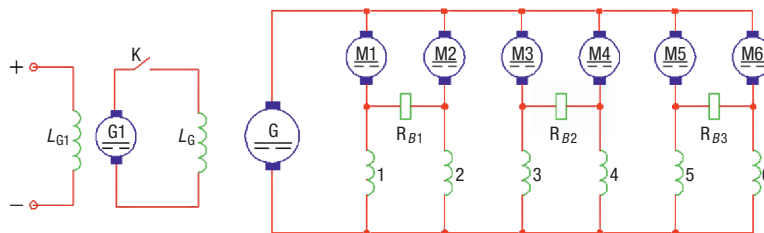


**Fig. 8.** A circuit diagram of the relay wheel-sets' slip and slide protection system in a conventional diesel-electric locomotive (of DC/DC type):  $G$  is a separately excited shunt-wound DC traction generator;  $G1$  is the exciter;  $L_G$  is the exciting winding of a DC traction generator;  $L_{G1}$  is the exciting winding of the generator's exciter;  $R_{B1}, R_{B2}, R_{B3}$  are the relays for controlling the process of the locomotive slipping; 1,..., 6 are the exciting windings of the DC traction motors.

$M1...M6$  are the DC traction motors,  $K$  is the contactor

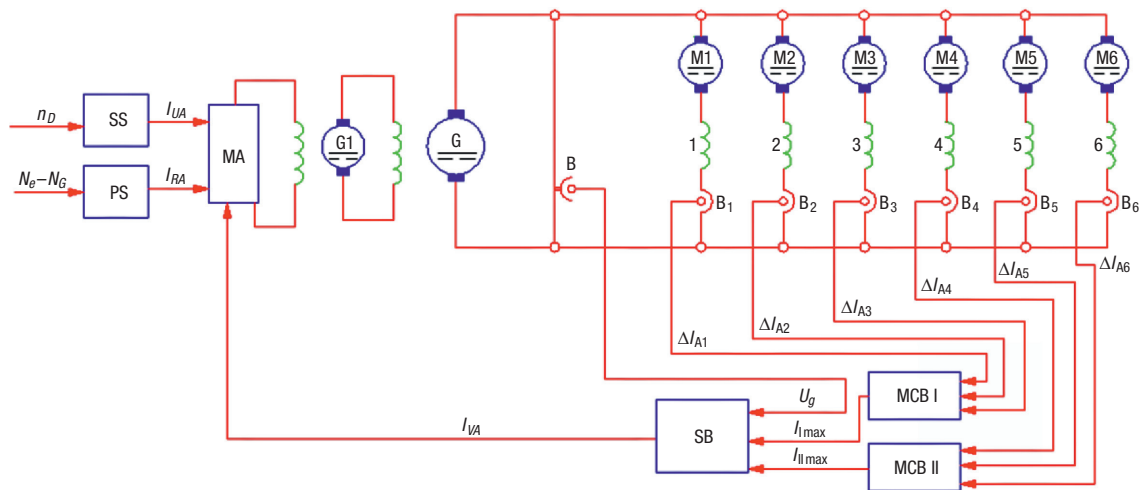


**Fig. 9.** A circuit diagram of automatic control of wheel-sets' slip and slide parameters in diesel-electric powered locomotive (of DC/DC type): G is a separately excited shunt-wound DC traction generator; G1 is the exciter; MA is a magnetic amplifier; B1, ..., B6 are armature current sensors of DC traction motors; M1, ..., M6 are series wound DC traction motors; PS is a diesel power sensor; SS is a diesel speed sensor; MCBI is the maximal current sensor block of traction motors of bogie I; MCBII is the maximal current sensor block of traction motors of bogie II; SB is a selective block; B is traction generator's voltage sensor;  $N_e$  is a signal of diesel motor's power;  $N_G$  is a signal of traction generator's power;  $n_D$  are revolutions (speed) of the diesel engine

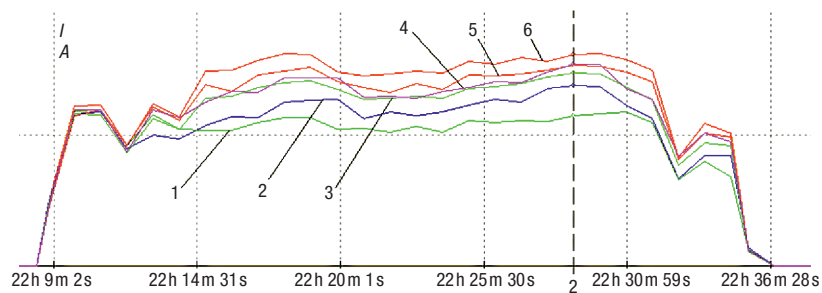


**Fig. 10.** The curves demonstrating the 'spread' in DC traction motors' armature current in the locomotive 2M62M: 1, ..., 6 are traction motors' armature currents, measured by a PC in testing trains of various masses

#### 4.4. The Suggested Algorithm for Automatic Control of Wheel-Sets' Slipping and Sliding

Based on the analysis of the anti-slip systems commonly used in DC/DC locomotives, the authors suggested a new automatic slipping protection system. This system ensures slip and slide monitoring and adjusting of the ABCD characteristic of the traction generator, when a signal about traction motor's armature current variation is obtained. It also creates a dynamic component of the dynamic characteristic, which is denoted by symbols  $E_1Y_1$  in the first curve of the characteristic and by symbols  $E_2Y_2$  in the second curve of the characteristic (see Fig. 11, coloured green).

The above formation of artificial characteristics of the locomotive, moving at some particular speed in the traction mode, allows us to maintain fixed voltage at the traction generator terminals for a very 'short' time (stabilizing it during the dynamic process), when the wheel-sets start slipping. In this case, it is possible to obtain the same speed of rotation of all traction motors' wheel-sets and, thereby, to regain proper adhesion of the wheels to the rails. When this is achieved, the previous

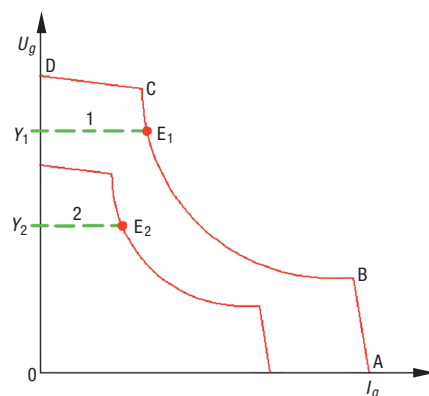


**Fig. 11.** Load characteristics of a diesel- electric powered locomotive's (of DC/DC type) traction generator  $U_g = f(I_g)$ : red denotes conventional characteristics; green show complementary dynamic characteristics; 1 and 2 show different locomotive drive regimes

value of the generator's voltage is automatically regained, i.e. it returns from the line YE to any CB portion of the artificial characteristic of the DC generator (Fig. 11, coloured red).

The straight-line locomotive's speed does not change during slipping and sliding because the suggested process of the dynamic control of the electric parameters is the fastest control method, since a transient process takes only a few milliseconds. The development of the tractive force of the locomotive is not interrupted because wheel-set slipping control is fully automated.

## 5. Conclusions

1. Taking into account the specific nature of the conventional characteristic of series excitation DC traction motors, slip and slide protection systems should be used to ensure uniform traction of locomotives.
2. Locomotive slip and slide protection systems, commonly used in the locomotives with series excitation DC motors are not effective because wheel-set slipping is controlled by the inertial relay systems. In this case, the development of the tractive force is interrupted during the process, which causes the development of the dynamic longitudinal tensile – compression forces in the train.
3. A locomotive's complementary slip and slide protection system suggested by the authors for the locomotives with series excitation DC traction motors, allows for automatic control of the traction generator's load characteristic, as well as the process of wheel-set slipping and sliding without interrupting the development of the tractive force of the locomotive, operating in the traction mode.
4. A locomotive's complementary wheel-sets' control system for the DC/DC locomotive allows us to change the nature (type) of traction generators' characteristics for the locomotives operating in the traction mode.
5. Using the suggested locomotive slip and slide protection system of the DC/DC locomotive wheel-sets, the driver does not have to interrupt the control of the traction mode; therefore, the development of longitudinal forces in the train is avoided.
6. The use of the suggested locomotive slip and slide protection system ensures optimal and steady tractive force control.
7. The suggested locomotive slip and slide protection system ensures an increasing of railway traffic safety and decreasing the wear/fatigue of the rails and wheel-sets as well as the maintenance and repair costs.

## References

- Andersson, E.; Berg, M.; Stichel, S. 2004. *Rail Vehicle Dynamics*. KTH Railway Technology. 600 p.
- Berthier, Y.; Descartes, S.; Busquet, M.; Niccolini, E.; Desrayaud, C.; Baillet, L.; Baitto-Dubourg, M. C. 2004. The role and effects of the third body in the wheel–rail interaction, *Fatigue & Fracture of Engineering Materials & Structures* 27(5): 423–436. doi:10.1111/j.1460-2695.2004.00764.x
- Braess, H. H.; Seiffert, U. 2011. *Vieweg Handbuch Kraftfahrzeugtechnik*. Vieweg+Teubner Verlag. 1036 p. (in German).
- Bucher, F.; Knothe, K.; Theiler, A. 2002. Normal and tangential contact problem of surfaces with measured roughness, *Wear* 253(1–2): 204–218. doi:10.1016/S0043-1648(02)00102-3
- Bureika, G. 2008. A mathematical model of train continuous motion uphill, *Transport* 23(2): 135–137. doi:10.3846/1648-4142.2008.23.135-137
- Chen, H.; Ban, T.; Ishida, M.; Nakahara, T. 2008. Experimental investigation of influential factors on adhesion between wheel and rail under wet conditions, *Wear* 265(9–10): 1504–1511. doi:10.1016/j.wear.2008.02.034
- Chen, H.; Ishida, M.; Nakahara, T. 2005. Analysis of adhesion under wet conditions for three-dimensional contact on side ring surface roughness, *Wear* 258(7–8): 1209–1216. doi:10.1016/j.wear.2004.03.031
- Ertz, M.; Bucher, F. 2003. Improved creep force model for wheel/rail contact considering roughness and temperature, in *Dynamics of Vehicles on Roads and on Tracks: Proceedings of the 17th IAVSD Symposium held in Lingby, Denmark, August 2001*. *Vehicle System Dynamics* Supplement 37: 314–325.
- Ertz, M.; Knothe, K. 2002. A comparison of analytical and numerical methods for the calculation of temperatures in wheel/rail contact, *Wear* 253(3–4): 498–508. doi:10.1016/S0043-1648(02)00120-5
- Harrison, H.; Mccanney, T.; Cotter, J. 2000. Recent developments in COF measurements at the rail/wheel interface, in *Proceedings of the Fifth International Conference Contact Mechanics and Wear of Rail Wheel Systems*, 25–28 July, 2000, Tokyo, Japan, 30–35.
- Hou, K.; Kalousek, J. 2000. Thermal effect on adhesion in wheel/rail interface, in *Proceedings of the Fifth International Conference Contact Mechanics and Wear of Rail Wheel Systems*, 25–28 July, 2000, Tokyo, Japan, 239–244.
- Hu, Y.-Z.; Zhu, D. 2000. A full numerical solution to the mixed lubrication in point contacts, *Journal of Tribology* 122(1): 1–9. doi:10.1115/1.555322
- Inarida, S.; Kojima, T.; Shimada, M.; Masuda, S. 2001. Train traction systems for passenger comfort and easier maintenance, *Hitachi Review* 50(4): 134–138. Available from Internet: <[http://www.hitachi.com/ICSFiles/afield-file/2004/06/08/r2001\\_04\\_103.pdf](http://www.hitachi.com/ICSFiles/afield-file/2004/06/08/r2001_04_103.pdf)>.
- Iwnicki, S. 2006. *Handbook of Railway Vehicle Dynamics*. 1st edition. CRC Press. 552 p.
- Kalker, J. J. 1967. *On the Rolling Contact of Two Elastic Bodies in the Presence of Dry Friction*: PhD Thesis. Delft University of Technology. 155 p. Available from Internet: <<http://repository.tudelft.nl/assets/uid:aa44829b-c75c-4abd-9a03-fec17e121132/P1219-6253.pdf>>.
- Kalker, J. J. 1982. A fast algorithm for the simplified theory of rolling contact, *Vehicle System Dynamics* 11(1): 1–13. doi:10.1080/00423118208968684
- Liudvinavičius, L.; Lingaitis, L. P. 2010. New locomotive energy management systems, *Maintenance and Reliability = Eksploatacija i Niezawodność* (1): 35–41.
- Myamlin, S. V. 2002. *Modelirovanije dinamiki rešovyh ekipazhej*. Dnepropetrovsk: Novaya ideologiya. 240 p. (in Russian).
- Mei, T. X.; Yu, J. H.; Wilson, D. A. 2009. A mechatronic approach for effective wheel slip control in railway traction, *Proceedings of the Institution of Mechanical Engineers, Part F: Journal of Rail and Rapid Transit* 223(3): 295–304. doi:10.1243/09544097JRR249
- Nayal, A.; Gupta, S. P.; Singh, S. P. 2006. Performance analysis of dc motor drive in electric traction with wheel slip control, *Journal of Institution of Engineers (India) – Part Electrical Engineering Division* 87: 55–60.



- Niccolini, E.; Berthier, Y. 2005. Wheel–rail adhesion: laboratory study of ‘natural’ third body role on locomotives wheels and rails, *Wear* 258(7–8): 1172–1178. doi:10.1016/j.wear.2004.03.028
- Nielsen, J. B.; Theiler, A. 1996. Tangential contact problem with friction coefficients depending on sliding velocity, in *Proceedings of the Second Mini Conference on Contact Mechanics and Wear of Rail/Wheel Systems*, 29–31 July 1996, Budapest, Hungary, 44–51.
- Ohyama, T. 1989. Some basic studies on the influence of surface contamination on adhesion force between wheel and rail at higher speeds, *Quarterly Report of RTRI* 30(3): 127–135.
- Ohyama, T.; Ohno, K.; Nakano, S. 1989. Influence of surface contamination on adhesion force between wheel and rail at higher speeds—behavior of adhesion force under the surfaces contaminated with a small amount of liquid paraffin, *Journal of JSLE – International Edition* 10: 111–114.
- Ohyama, T.; Maruyama, H. 1982. Traction slip at higher rolling speeds: some experiments under dry friction and water lubrication, in *Proceedings of the 1st International Conference on Contact Mechanics and Wear of Rail/Wheel Systems*, 395–418.
- Patir, N.; Cheng, H. S. 1978. An average flow model for determining effects of three-dimensional roughness on partial hydrodynamic lubrication, *Journal of Lubrication Technology* 100(1): 12–17. doi:10.1115/1.3453103
- Polach, O. 2005. Creep forces in simulations of traction vehicles running on adhesion limit, *Wear* 258(7–8): 992–1000. doi:10.1016/j.wear.2004.03.046
- Polach, O. 2001. Influence of locomotive tractive effort on the forces between wheel and rail, in *Selected Papers from the 20th International Congress of Theoretical and Applied Mechanics held in Chicago, USA, 28 August–1 September, 2000*, *Vehicle System Dynamics Supplement* 35: 7–22.
- Polach, O. 1999. A fast wheel–rail forces calculation computer code, *Vehicle System Dynamics Supplement* 33: 728–739.
- Polach, O. 1992. Solution of wheel–rail contact forces suitable for calculation of rail vehicle dynamics, in *Proceedings of the Second International Conference on Railway Bogies*, 14–16 September 1992, Budapest, 10–17.
- Program 2011/12 – High Precision Drives and Systems*. Available from Internet: <<http://www.maxonmotor.ch/e-paper>>.
- Radojković, B. 1990. *Električna vuča*. Beograd: Naucna knjiga. 468 p. (in Serbian).
- Sen, P. C. 1996. *Principles of Electric Machines and Power Electronics*. 2nd edition. John Wiley & Sons, Inc. 640 p.
- Sextro, W. 2010. *Dynamical Contact Problems with Friction: Models, Methods, Experiments and Applications*. Springer. 200 p.
- Strekopytov, V. V.; Gryschenko, A. V.; Kruchek, V. A. 2003. *Elektricheskije peredachi lokomotivov*. Moskva: Marshrut. 305 p. (in Russian).
- Tomberger, C.; Dietmaier, P.; Sextro, W.; Six, K. 2011. Friction in wheel–rail contact: a model comprising interfacial fluids, surface roughness and temperature, *Wear* 271(1–2): 2–12. doi:10.1016/j.wear.2010.10.025
- Wickens, A. H. 2003. *Fundamentals of Rail Vehicle Dynamics*. 1st edition. Taylor & Francis. 295 p.
- Yamaguchi, J. 2006. Blue skies at Makuhari, *Automotive Engineering International* 1: 55–62.
- Zhang, W.; Chen, J.; Wu, X.; Jin, X. 2002. Wheel/rail adhesion and analysis by using full scale roller rig, *Wear* 253(1–2): 82–88. doi:10.1016/S0043-1648(02)00086-8